Applied Catalysis B: Environmental 132–133 (2013) 527–534

Contents lists available at SciVerse ScienceDirect

Applied Catalysis B: Environmental

journal homepage: www.elsevier.com/locate/apcatb

Review

Carbon–NSR catalyst interaction: Impact on catalyst structure and NO_x storage efficiency

Jennifer Klein[a], Dongliang Wu[a], Valerie Tschamber[a,*], Ioana Fechete[b], Francois Garin[b]

[a] Laboratoire Gestion des Risques et Environnement, Université de Haute Alsace, 3b rue A. Werner, 68093 Mulhouse Cedex, France
[b] Laboratoire des Matériaux, Surfaces et Procédés pour la Catalyse, Université de Strasbourg, UMR 7515 CNRS, 25 rue Becquerel, 67087 Strasbourg Cedex 2, France

ARTICLE INFO

Article history:
Received 26 September 2012
Received in revised form
14 December 2012
Accepted 18 December 2012
Available online 24 December 2012

Keywords:
NO_x storage capacity
Soot
Sintering
Platinum based catalyst
Barium nitrate

ABSTRACT

The impact of the presence of carbon on the structure of model NO_x storage catalysts (NSR) and their ability to store NO_x were investigated. Three catalysts, composed of Pt and/or Ba supported on Al_2O_3, were prepared. Reactivity of the catalysts toward NO_x storage was studied during adsorption/TPD cycles. Comparison of the results obtained in the presence and absence of carbon in the catalytic bed revealed that a carbon–catalyst contact leads to a decrease in NO_x storage capacity attributed to a destabilization of nitrate species formed far from Pt sites. Both Al and Ba sites are affected. During the carbon oxidation process, an aging of the catalysts, caused by Pt sintering and Ba agglomeration, as observed using TEM technology. These structural modifications reduce the proximity between the Pt sites and adsorption sites (Ba and/or Al), which results in a decrease in the NO_x storage toward the 'nitrite route'.

Contents

1. Introduction

The use of after-treatment devices to reduce NO_x and soot emissions generated by diesel engines is currently mandatory to meet European standards. To control soot emissions, diesel particulate filters (DPF) are typically used. This technology traps soot, which must then be removed to maintain filtration capacity. Regeneration of the filter, which is the crucial step of this technology, is usually based on the oxidation of deposited soot either by O_2 and/or by the gas mixture NO_2/O_2. When using O_2 as oxidant, the presence of a ceria-based catalyst, associated with the soot particles and/or deposited on the filter walls, is necessary to achieve a sufficient gasification rate. To improve this rate even further, a periodical extra-fuel injection is usually performed so that the exhaust gas temperature increases. However, this process leads to excess fuel consumption. As NO_2 is a better oxidant than O_2, its presence in the gas flow allows soot oxidation at a lower temperature (above 250 °C) [1–3]. Thus, with a gas stream composed of a mixture of NO_2

* Corresponding author. Tel.: +33 03 89 33 61 58; fax: +33 03 89 33 61 61.
E-mail address: valerie.tschamber@uha.fr (V. Tschamber).

0926-3373/$ – see front matter © 2013 Elsevier B.V. All rights reserved.
http://dx.doi.org/10.1016/j.apcatb.2012.12.019

and O_2, continuous soot combustion in the filter can be obtained in the average temperature range of diesel exhaust (300–400 °C) [4–6]. However, because NO_2 is present in the diesel exhaust stream at a low concentration (5–15% of total NO_x), a diesel oxidation catalyst (DOC), placed upstream of the particulate filter or as a coating on the channel walls of the diesel particulate filter, is necessary to oxidize NO to NO_2. The DOC generally implemented is a Pt-based catalyst. Such a process was used in the continuous regeneration trap (CRT) technology proposed by Johnson Matthey [7]. The mechanism involved in the oxidation of soot by a NO_2/O_2 mixture is now well established and consists of two main reactions occurring simultaneously: a direct reaction between carbon and NO_2 and a cooperative reaction simultaneously involving O_2 and NO_2 [3,6]. In the latter case, NO_2 adsorbs on —C(O) complexes resulting from O_2 chemisorption to form nitro-oxygenated intermediate species, which are then decomposed by NO_2 [6,8]. Both the direct and the cooperative reactions lead to carbonaceous material combustion with CO_2 and CO formation and NO_2 reduction to NO. Several studies performed at a laboratory scale revealed that when soot is in contact with the DOC, an enhancement of the cooperative reaction rate occurs. Jeguirim et al. [9,10] proposed that besides the well-known catalytic reoxidation of NO into NO_2, Pt also exerts a catalytic effect on the cooperative carbon–NO_2–O_2 oxidation reaction. It acts on the cooperative reaction by enhancing the formation of atomic oxygen, which is then transferred to the carbon surface.

Two different technologies were developed to reduce NO_x emission in an oxygen-rich environment: selective catalytic reduction (SCR) and NO_x storage reduction (NSR). The latter technology is more suited for passenger cars and works under cyclic conditions alternating lean periods during which NO_x is stored as nitrate on the catalyst and shorter rich periods during which nitrates are desorbed and reduced to N_2. The behavior of NSR catalysts or model NSR catalysts, such as Pt–Ba/Al_2O_3, Pt–K/Al_2O_3 or Pt–K–Ba/Al_2O_3, is well documented in the literature. In the last decade, several papers have focused on the NO_x storage mechanism [11–14]. It is generally admitted that the first stage consists of the oxidation of NO into NO_2 on platinum (Pt) sites. Olsson et al. [11] proposed that NO_2(g) is then loosely bound to BaO sites, leading to the formation of BaO–NO_2 intermediaries that decompose on BaO_2 to release NO(g). This step is then followed by nitrate formation resulting from the adsorption of NO_2 gas on BaO_2 sites. Previously, Mazhoul et al. [13] concluded that Pt sites close to barium sites allow nitrate formation, while Pt sites far from barium sites are responsible for NO oxidation. Nova et al. [12] recently proposed, in accordance with these results, a more detailed mechanism with two distinct routes: a 'nitrite route' and a 'nitrate route'. The 'nitrite route' implies the oxidation of NO on Pt sites followed by the formation of nitrite ad-species on Ba neighboring Pt sites. Nitrite ad-species are then progressively oxidized into nitrate species, which prevail at saturation. Accordingly, a cooperative interaction between Pt and a nearby Ba site is important for this route and Pt plays a role in both the formation of nitrites and their subsequent oxidation to nitrates. Conversely, the 'nitrate route' corresponds to NO_2 storage on BaO, directly in the form of nitrates without proximity between the Ba and Pt sites. This route implies the release of one NO molecule for three molecules of NO_2 consumed. Nova et al. [12] proposed that both the 'nitrite' and 'nitrate' routes occur simultaneously during NO/O_2 storage.

To decrease the size of the after-treatment devices assembled along the exhaust line and the induced backpressure, Toyota [15] developed the diesel particulate NO_x reduction (DPNR) system. This system is composed of a particulate wall-flow filter coated with an NSR catalyst layer and works under cyclic conditions. Particulate filter regeneration is supposed to be effective during the lean phase due to the presence of NO_x and the excess of oxygen in the exhaust gas, similarly to CRT technology. It is also claimed that soot oxidation occurs during the rich phase [15]. Then, soot treatment, NO_x reduction and CO and hydrocarbon oxidation functions are coupled on a single monolith, leading to this technology being named a '4-way catalytic converter'. Combination of NSR and CRT technologies modifies their behavior, so recent studies have investigated the reaction mechanism of 4-way catalytic materials [16–23]. Most of these investigations were focused on the influence of the presence of a model NSR catalyst (Pt–Ba/Al_2O_3 or Pt–K/Al_2O_3) on soot oxidation and concluded that NO_x storage function enhanced soot combustion either by decreasing the soot oxidation temperature and/or by increasing the local NO_2 gas phase concentration [17,20–22]. While several authors [18–23] observed that the NO_x storage capacity of the NSR catalyst was partially inhibited by the presence of soot, only a few of them [18,19,22,23] investigated the soot–NSR catalyst interaction and its influence on the NO_x storage mechanism. In our previous work, participation of the following direct surface reaction between carbon particles and NO_x storage sites to form adsorbed carbonate species was proposed:

$$C* + Ba(NO_3)_2 \rightarrow BaCO_3 + 2NO + (1/2)O_2 + * \quad (1)$$

$$Al(NO_3)_3 + 3C* \rightarrow Al_2(CO_3)_3 + 6NO + (3/2)O_2 + * \quad (2)$$

Our results showed that carbon contact with the NO_x storage catalyst affects nitrate species formed by the 'nitrate route' (far from Pt sites) more than those formed by the 'nitrite route'.

The purpose of this study was to investigate more precisely the effect of the interaction between carbon and model NSR catalysts on both the catalyst structure and its NO_x storage capacity. The catalysts used were model catalysts composed of Pt and/or Ba on Al_2O_3. For this purpose, the activity of the materials toward NO_x storage was measured in a fixed bed reactor at 300 °C in the presence and absence of carbon black in the catalytic bed. The effect of aging induced by contact with carbon black on catalyst NO_x storage capacity was studied. TEM characterization was also performed.

2. Experimental

2.1. Materials preparation

The 2 wt.%Pt/γ-Al_2O_3 (noted Pt/Al_2O_3) and 20 wt.%BaO/γ-Al_2O_3 (noted Ba/Al_2O_3) catalysts were prepared by wet impregnation of alumina (Alfa Aesar, 220 m^2/g) with a solution of platinum (II) acetylacetonate (Alfa Aesar, Pt 48% min) (8.2 g/L in ethanol 4 vol/dichloromethane 1 vol) or an aqueous solution of barium nitrate (Fluka, 99% purity) (70 g/L), respectively. The preparation of the 2%Pt–20%BaO/γ-Al_2O_3 (noted Pt–Ba/Al_2O_3) catalyst involve the impregnation of alumina with the barium nitrate solution then with the platinum acetylacetonate solution. After drying in air at 383 K during 14 h, the catalysts were calcined at 973 K for 2 h under 20% b.v. O_2 in N_2.

A commercial carbon black (CB), Vulcan 6 from Cabot with a specific surface area equal to 106 m^2/g, was used as a model for soot particles.

2.2. Reactivity tests

The catalytic activity of the different catalysts for NO_x adsorption and carbon oxidation was measured using a fixed bed quartz reactor (internal diameter 16 mm) placed in the experimental set up described in Ref. [18]. Catalytic tests were performed either with pure catalyst or in the presence of a carbon–catalyst mixture. Catalytic tests with pure catalyst were carried out on a sample of 1.2 g in the reactor. For the experiments performed in the presence of the carbon–catalyst mixture, 200 mg of carbon black, prepared as described in [18], was physically mixed with 1.2 g of catalyst with

a spatula in order to obtain a loose contact between the two materials (carbon black and catalyst). A loose contact was preferred in this work in order to be representative to the contact, which occurs in real operating conditions. The NO_x storage capacity of the materials was studied by performing isothermal NO_x adsorption/temperature programmed desorption (TPD) cycles according the procedures (pre-treatment and stabilization) described in [18]. The adsorption phase was performed at 300 °C with a reactive gas mixture (60 N L h^{-1}) containing 300 ppmv NO + 10% b.v. O_2 in N_2 or 300 ppmv NO_2 + 10% b.v. O_2 in N_2. TPD was carried out under pure N_2 from 573 K to 873 K (rate 5°/min). The outlet gas was analyzed using an infrared ROSEMOUNT NGA 2000 analyzer to quantify the outlet NO, NO_2, CO and CO_2 molar fractions.

The samples (catalyst or carbon–catalyst mixture) have been conditioned by performing four NO_x adsorption/TPD cycles in order to obtain a reproducible behavior. Note that each NO_x adsorption/TPD cycle were separated by the reducing surface treatment under 2%H_2 in N_2 at 573 K. In the following sections, the samples conditioned by four NO_x adsorption/TPD cycles in absence of carbon will be named 'conditioned' samples.

At the end of the fourth cycle, performed in presence of carbon, the carbon/catalyst mixture was cooled to 490 °C under pure N_2 and then a gas mixture containing 10% b.v. O_2 in N_2 was injected to oxidize the carbon in the sample. The temperature was maintained at 490 °C for 30 min and then slowly raised to 600 °C (1 °C/min) so that a controlled oxidation of carbon was maintained without any large exothermicity. The sample was then maintained at this temperature to fully oxidize all of the carbon. The total oxidation of the remaining carbon after the four successive adsorption/TPD cycles was controlled by a carbon balance calculated from CO and CO_2 emissions measured at the outlet of the reactor during this oxidative treatment. Subsequently, the sample was cooled to 300 °C under N_2, and the catalyst was reduced under 2% (v/v) H_2 in N_2. One NO_x adsorption/TPD cycle was then performed under the same conditions as described above. We can note here that no CO or CO_2 emission was detected during this cycle, which confirms that the oxidative treatment at 600 °C allowed a total combustion of carbon (i.e., no carbon was present yet in the reactor). Catalyst samples obtained after this last NO_x adsorption/TPD cycle were named 'aged' samples.

2.3. Characterization techniques

Surface area and porous properties of 'conditioned' and 'aged' samples were determined by nitrogen adsorption at −196 °C on a TriStar apparatus. Prior to the sorption (adsorption–desorption) measurements, the samples were out-gassed overnight at 150 °C. The specific surface area was calculated using the standard Brunauer–Emmett–Teller (BET) method. The total pore volume was estimated from the amount of nitrogen adsorbed at a relative pressure, p/p_0, of 0.99, assuming complete surface saturation with nitrogen and where p and p_0 denote the equilibrium pressure and saturation vapor pressure, respectively. Results are presented in Table 1.

Table 1
Surface area and porous properties of conditioned and aged samples.

Catalyst	Surface area (m^2/g)	Pore volume (cm^3/g)
Al_2O_3		
Conditioned	188	0.60
Aged	184	0.58
Ba/Al_2O_3		
Conditioned	148	0.43
Aged	135	0.41
Pt/Al_2O_3		
Conditioned	190	0.57
Aged	187	0.58
$Pt/Ba/Al_2O_3$		
Conditioned	143	0.41
Aged	136	0.41

Transmission electron microscopy (TEM) images of 'conditioned' and 'aged' samples were obtained on a Topcon 2100 FCs microscope operating at 200 kV. The samples were dispersed in ethanol in an ultrasonic bath for several minutes, and then deposited on a Cu grid and dried at room temperature.

3. Results and discussion

3.1. NO_x adsorption in presence of carbon black

The NO_x storage capacities (NSC) of the carbon–catalyst mixtures measured during the four successive adsorption/TPD cycles are shown in Table 2. In this table is also reported the NSC of the conditioned catalysts, measured in absence of carbon black in the reactor. The NSC of the carbon–catalyst mixtures measured during the first cycle (cycle 1) is lower than the one measured on conditioned catalysts regardless of the composition of catalyst. This result is in agreement with the one reported in a previous work [18]. Thus, the loss of NSC when carbon is present in the reactor in loose contact with the catalysts is attributed to the formation of carbonate species according to surface reactions (1) and (2).

The following successive adsorption/TPD cycles show an evolution of NSC. This one is depending on the catalyst composition. NO_x storage capacity on alumina remains almost stable with the presence of carbon black which inhibits NO_x storage by close to 40%. Conversely, the efficiency of the carbon–Ba/Al_2O_3 mixture is greatly enhanced between the first cycle and subsequent ones. Thus, the inhibiting effect of carbon black on NSC for Ba/Al_2O_3 catalyst decreases from 55% to 30% between the first and the second cycle. The NSC measured on the carbon–Ba/Al_2O_3 mixture remains then almost unchanged after the second cycle and, as for alumina catalyst, is lower than the NSC observed in the absence of carbon. The evolution of NSC of the Pt-free catalysts during the successive experiments is indicative of a decrease in the interactions between the carbon and the catalyst. This one can be firstly attributed to

Table 2
NO_x storage capacities (NSC) of conditioned catalysts and carbon–catalyst mixtures during the 4 successive adsorption/TPD cycles.

Catalyst	Gas composition	NSC (μmol/g_{cat})				
		Pure catalyst	Carbon–catalyst mixture			
		Cycle 4	Cycle 1	Cycle 2	Cycle 3	Cycle 4
Al_2O_3	NO_2/O_2	210	120	125	140	135
Ba/Al_2O_3	NO_2/O_2	430	195	305	310	285
Pt/Al_2O_3	NO/O_2	140	140	145	120	110
	NO_2/O_2	200	165	160	145	140
$Pt/Ba/Al_2O_3$	NO/O_2	500	430	390	400	390
	NO_2/O_2	560	500	440	390	390

the progressive combustion of carbon during the successive experiments, which decreases the carbon on catalyst ratio in the reactor. However, the carbon combustion during one cycle is low as it equals to about 20 mg. The different evolutions of NSC, observed between Ba/Al_2O_3 and alumina catalysts, suggest moreover that the participation of reaction (1) decreases during the successive experiments while those of reaction (2) is not impacted. Previous works on the mechanisms involved in the NO_x storage on Ba-based catalysts suggested that barium nitrates are rather mobile on the surface [24,25]. A modification of the surface of the Ba/Al_2O_3 catalyst and particularly of the Ba particles and their proximity with carbon can occurs and may also be at the origin of the observed results. This point will be discussed in Section 3.3.

The behavior of Pt-based catalysts during the successive experiments in presence of carbon differs from those obtained on Pt-free catalysts (Table 2). The NSC of Pt/Al_2O_3 catalyst progressively decreases with the adsorption/TPD cycles, independently of the reactive gas mixture composition (NO or NO_2). The presence of barium together with platinum, however, seems to stabilize the progressive loss in NO_x storage, particularly in the presence of NO. The fundamental role of Pt in the NSR catalysts is to allow the oxidation of NO into NO_2 and the spillover of NO_x from Pt to BaO, leading to the formation of surface nitrate species. The observed decrease of the NSC during the successive adsorption/TPD cycles, in presence of carbon on Pt-based catalysts, can be attributed to a modification of the surface structure of the catalyst either in terms of the size and dispersion of platinum particles (thus of the number of adsorption sites) or by a poisoning of Pt sites by carbon. The surface modification is depending on the presence or not of barium. This point will be detailed in Section 3.3.

3.2. NO_x desorption (TPD) in presence of carbon black

Fig. 1 compares the NO_x emissions obtained during TPD on conditioned catalysts (so in the absence of carbon) with those obtained during the first cycle on carbon–catalyst mixtures. One may observe that in all cases, the temperature at which the maximum desorption of NO_x occurs is lower in the presence of a carbon–catalyst mixture. This decrease in temperature was particularly important for Pt-free catalysts (Al_2O_3 and Ba/Al_2O_3), as in the case of Ba/Al_2O_3 where it is equal to 100 K. Using the Pt/Al_2O_3 catalyst, the effect of the carbon–catalyst contact on the maximum NO_x desorption temperature is more significant when NO_2 is injected in the gas mixture during the adsorption phase than using NO. This phenomena is less important using $Pt–Ba/Al_2O_3$ catalyst. The observed decrease in the NO_x desorption temperature

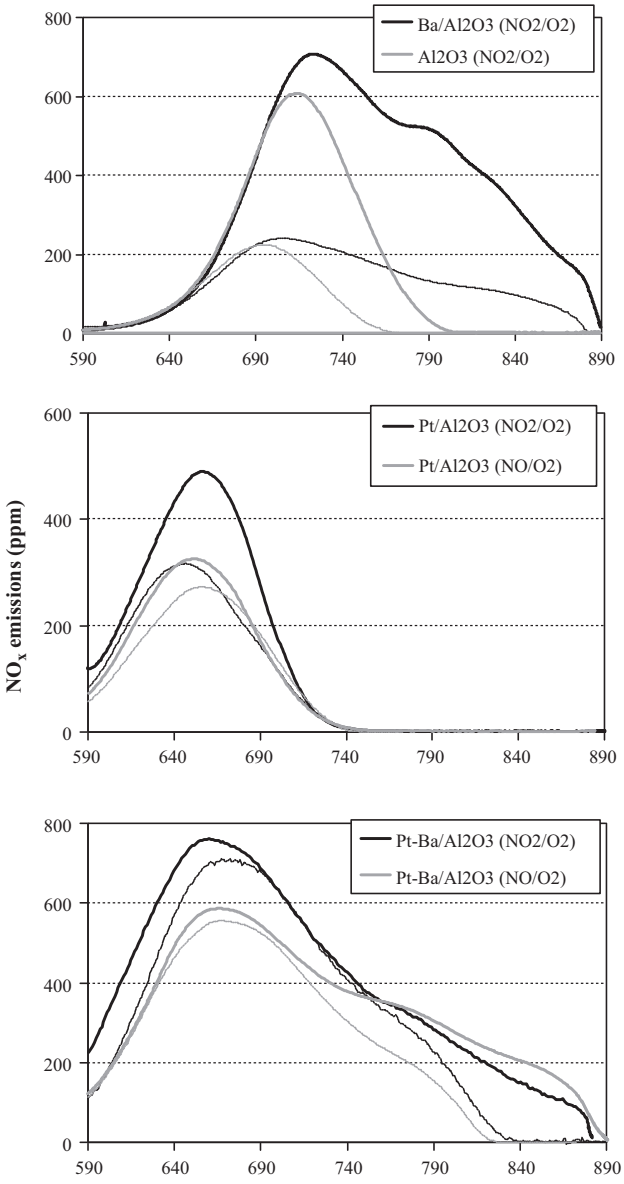

Fig. 1. Outlet NO_x concentration versus temperature during the TPD over conditioned catalysts (thick line) and carbon–catalyst mixtures (thin line).

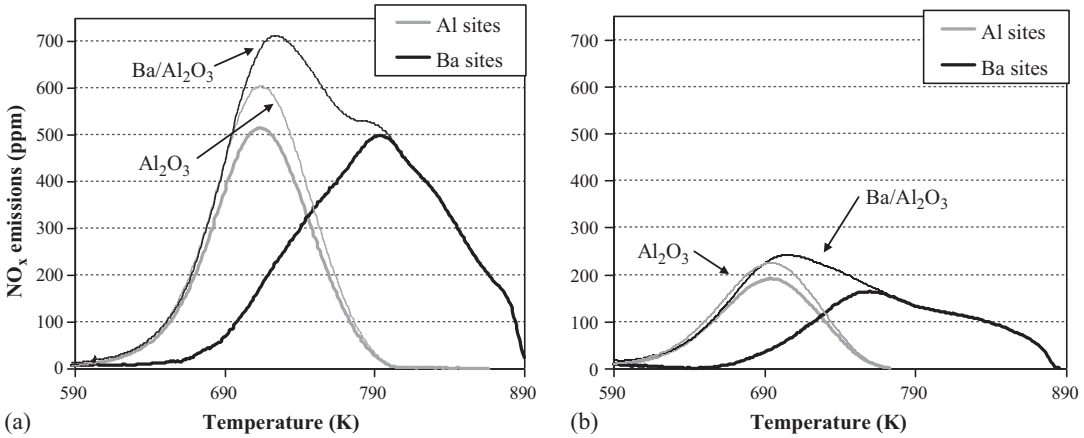

Fig. 2. Outlet NO_x concentration during the TPD versus temperature over Pt free catalysts (Al_2O_3 and Ba/Al_2O_3) (thin lines) and deconvolution of the TPD signal obtained on Ba/Al_2O_3 catalyst (thick lines) (a) in absence and (b) in presence of carbon black.

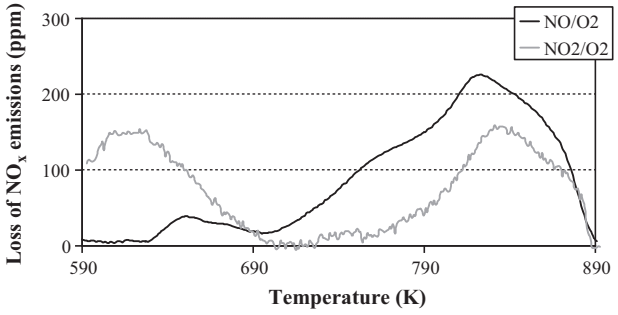

Fig. 3. Difference between NO_x emissions measured during the TPD, versus temperature, obtained over $Pt/Ba/Al_2O_3$ in absence and in presence of carbon black as a function of the reactive gas composition (300 ppmv NO or NO_2; 10% b.v. O_2; 60 N L h^{-1}).

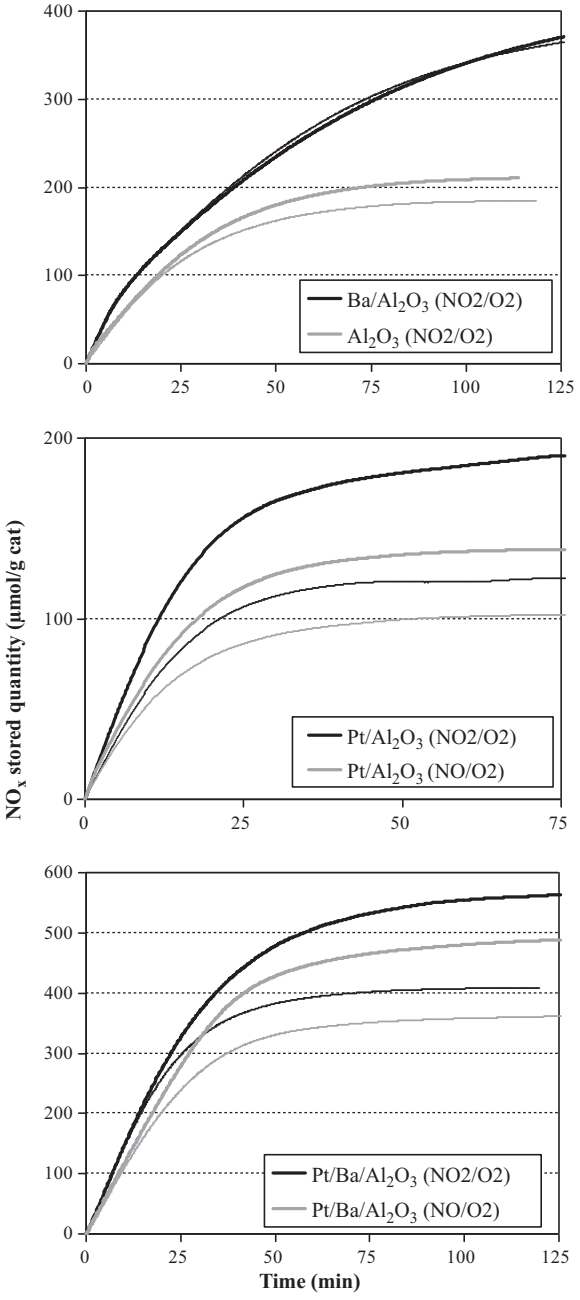

Fig. 4. Amount of adsorbed NO_x versus time over conditioned catalysts (thick line) and aged catalysts (thin line) (both are carbon-free) as a function of the reactive gas composition (300 ppmv NO or NO_2; 10% b.v. O_2; 60 N L h^{-1}).

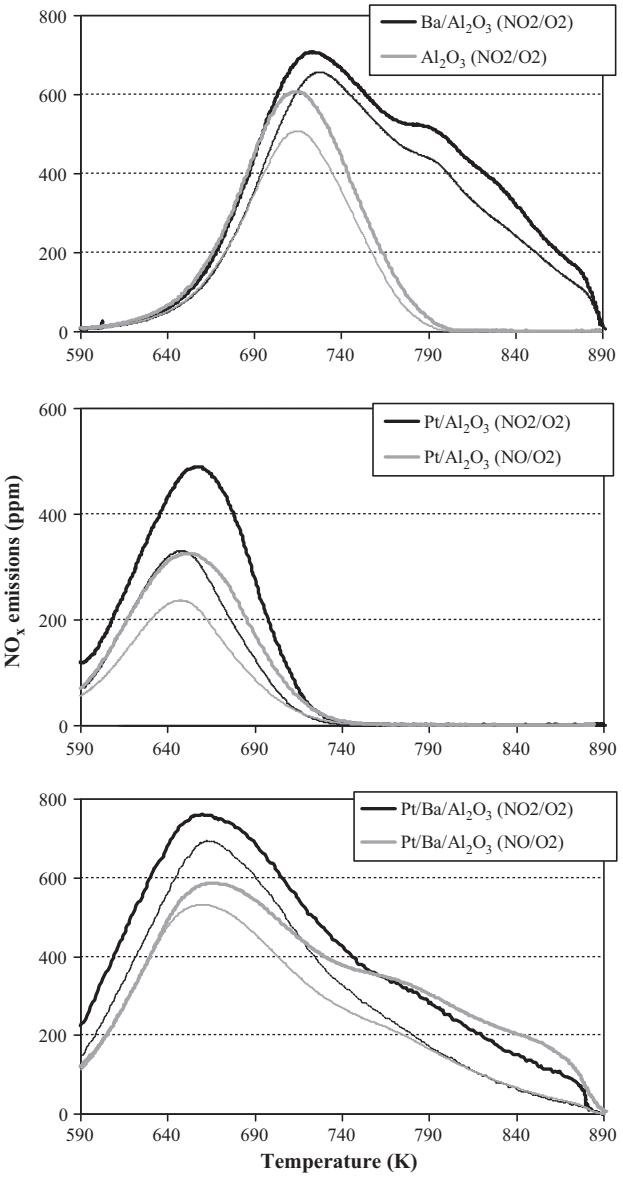

Fig. 5. Outlet concentration of NO_x obtained during the TPD versus temperature over conditioned catalysts (thick line) and aged catalysts (thin line) (both are carbon-free) as a function of the reactive gas composition during the absorption phase (300 ppmv NO or NO_2; 10% b.v. O_2; 60 N L h^{-1}).

reveals, as already proposed in previous works [18,26], that carbon black promotes the decomposition of stored nitrates. According to Sanchez et al. [26], in presence of soot a direct reaction between soot and adsorbed nitrate species occurs on the catalyst surface during the desorption of nitrate species.

Fig. 1 reveals too that the presence of carbon in the catalytic bed induced a strong modification of the shape of the TPD profiles above 750 K for experiments performed with catalysts composed of barium. It is important to note here that the nitrogen balance from the quantity of NO_x adsorbed during the lean phase and NO_x desorbed during TPD was obtained for experiments performed in the absence of carbon black. This balance was, however, not obtained when carbon is present in the reactor. Hence, the amount of NO_x ($NO + NO_2$) desorbed during the TPD corresponds to 90% and 80% for Pt/Al_2O_3 and Ba-based catalysts (Ba/Al_2O_3 and $Pt–Ba/Al_2O_3$), respectively, of the amount stored during the adsorption phase. Therefore, in the presence of carbon, a non-negligible amount of stored NO_x was reduced during the TPD.

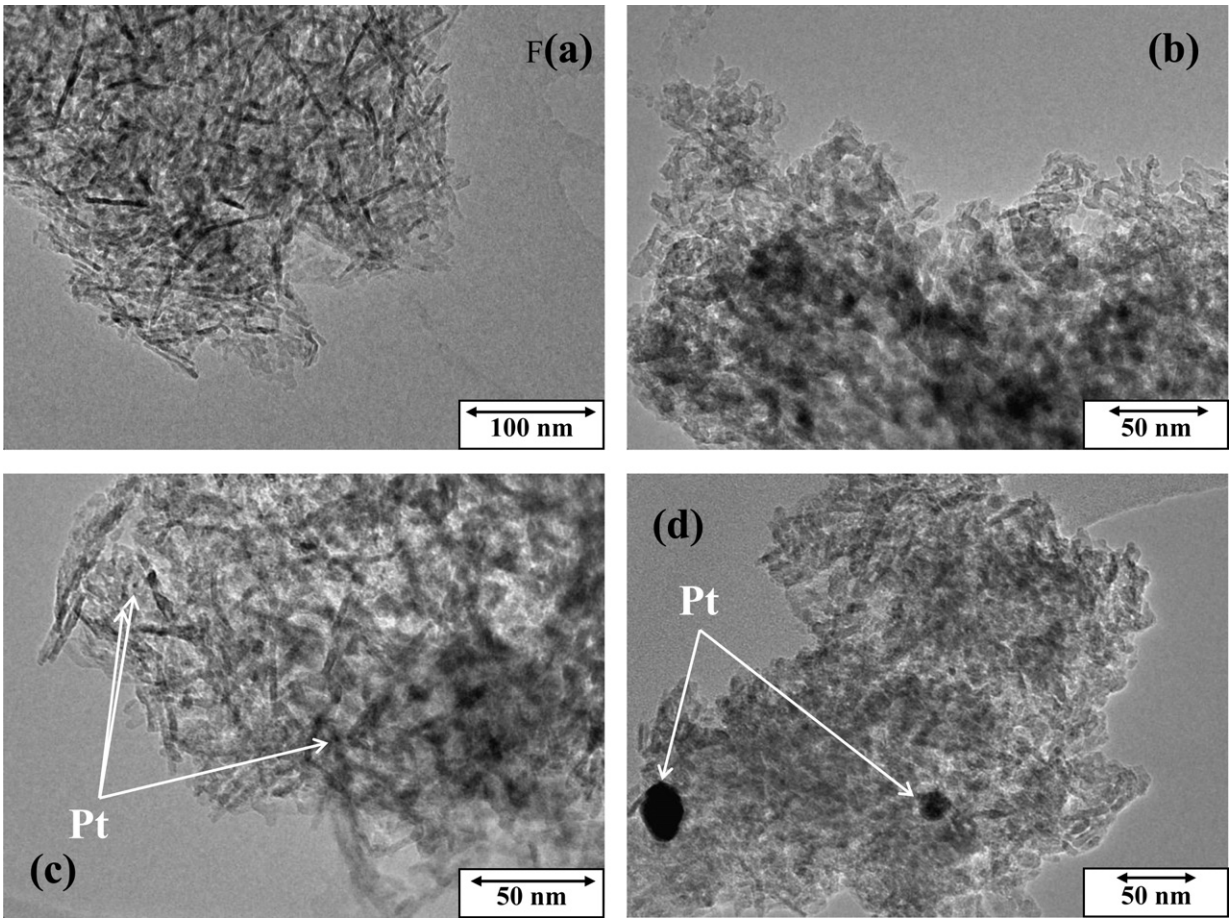

Fig. 6. TEM images of conditioned (a) and aged (b) Al_2O_3 and conditioned (c) and aged (d) Pt/Al_2O_3 catalyst.

To clarify the impact of the interaction between carbon and catalyst on NO_x storage sites, Fig. 2 presents the deconvolution of the TPD signal obtained on the Ba/Al_2O_3 catalysts alone and mixed with carbon. The deconvolution was made from the NO_x emission signal obtained during the TPD on Al_2O_3 material, and taking into account the BaO content in the Ba/Al_2O_3 catalyst. This deconvolution highlights that the NO_x storage on Ba/Al_2O_3 catalyst takes place on two distinctive sites: alumina and barium with a contribution of 40% and 60%, respectively (Fig. 2a). NO_x species adsorbed on barium site are obviously more stable than the ones adsorbed on alumina sites. The deconvolution of the NO_x emission signal obtained during the TPD for the carbon–Ba/Al_2O_3 mixture (Fig. 2b) shows that even if both adsorption sites are affected by the presence of carbon, the deactivation of the NO_x storage function is more important for the Ba storage sites than for the Al sites. Indeed, NO_x storage on Al sites decreases of 43%, as it decreases of 62% for Ba sites. This finding, associated with a more important destabilization of adsorbed nitrate species on Pt-free catalysts and/or when NO_2 is injected in the reactive gas during the adsorption phase instead of NO (see above) leads us to conclude that the carbon–catalyst contact inhibits nitrate species formed far from Pt sites (via the 'nitrate route') more than those vicinal to Pt sites (formed by the 'nitrite route'). This finding was consistent with our previous results [18].

Fig. 3 presents the difference between NO_x emissions obtained during the TPD, performed after an adsorption phase with NO/O_2 or NO_2/O_2 as reactive gas, on $Pt–Ba/Al_2O_3$ catalyst alone and mixed with carbon (i.e., the deficit in NO_x desorption when carbon was in contact with the catalysts). In relation with Fig. 2, it is clear from Fig. 3 that, in the same way to what observed for Pt-free catalyst, the two stored NO_x species (on Al and Ba sites) are influenced by the presence of carbon. On $Pt–Ba/Al_2O_3$ catalyst, species stored on Al sites are significantly more impacted when NO_2 was used as the reactive gas instead of NO. On the other hand, the deficit in NO_x observed during the TPD at higher temperature (Fig. 3) is attributed to both an inhibition of NO_x storage on barium sites and a reduction of stored NO_x during their desorption according to the following equation:

$$CO + 2NO \rightarrow 2CO_2 + N_2 \quad (3)$$

where CO comes from the oxidation of carbon by adsorbed oxygen, in accordance with CO_2 signal measured during the TPD (not show here).

3.3. Effects of soot on catalyst structure and NO_x storage capacity

3.3.1. Reactivity tests on aged samples

Fig. 4 compares the evolution of NO_x stored over time on conditioned (thick line) and aged (thin lines) catalyst samples as a function of the composition of the reactive gas. The NO_x storage rate of the Ba/Al_2O_3 catalyst measured during the first 2 h of exposure to the reactive gas is similar for both samples. For Al_2O_3, a common NO_x adsorption rate for conditioned and aged samples is obtained during the first 18 min of exposure. Then, the rate of adsorption for the aged sample decreases so that the NSC of this sample at saturation is less than 12% of that of the conditioned catalyst. Unlike Pt-free catalysts, Pt/Al_2O_3 and $Pt–Ba/Al_2O_3$ are more strongly affected by aging, with a loss of NSC noticeable within minutes of exposure to the reactive flow (27% and 38%, respectively, in the presence of NO_2/O_2). From these experimental data, one might conclude that, regardless of the catalysts composition and the reactive

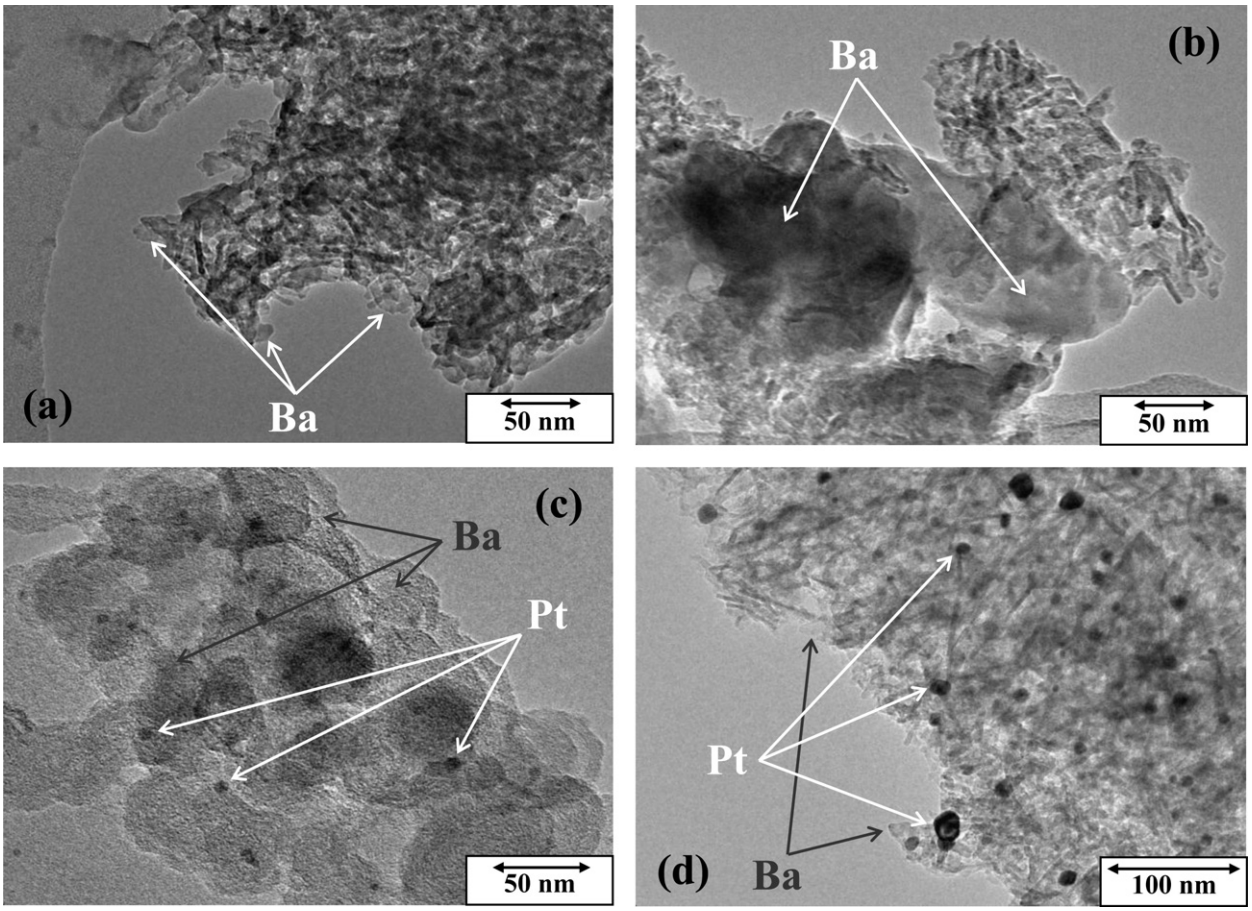

Fig. 7. TEM images of conditioned (a) and aged (b) Ba/Al_2O_3 catalyst and conditioned (c) and aged (d) $Pt–Ba/Al_2O_3$ catalyst.

gas, a decrease in NSC is observed on aged samples (i.e., after the soot has been burned). Thus, the inhibiting effect of the presence of carbon black on the NSC, observed when a carbon–catalyst contact is present in the reactor bed (Sections 3.1 and 3.2), induces irreversible modifications to the catalyst NSC, after a total soot combustion. Indeed, Pt-based catalysts lost more than a quarter of their initial storage capacity. For the following discussion, it is important to mention that the NO/NO_2 ratio measured at saturation was the same on both conditioned and aged samples for a defined catalyst.

TPD profiles measured on conditioned and aged samples are presented in Fig. 5. Unlike what was observed in the presence of the carbon–catalyst mixture (Fig. 1), NO_x desorption observed on aged samples is the same as on conditioned samples in terms of both shape and temperature. Thus, NO_x stored species stability is not affected by the aging treatment. It seems therefore that deactivation in NSC observed on aged catalysts is more the consequence of modification of the surface structure, and thus a fewer adsorption sites, than a modification of the NO_x adsorption mechanism.

3.3.2. *Materials characterization*

Transmission electron microscopy (TEM) images of conditioned and aged samples are compared (Figs. 6 and 7). As observed in Fig. 6a and b, Al_2O_3 appeared as nanowires with a cross-section of 2–4 mm. Aging do not substantially affects its structure even though the length of the filaments slightly decreased. For Pt/Al_2O_3 samples (Fig. 6c and d), a significant increase is observed in the mean platinum particle diameter from 2 nm on conditioned samples to 20 nm on the aged ones. A large dispersion in the platinum particle size is observed on the latter sample, reaching up to 40 nm. TEM images obtained on Ba/Al_2O_3 clearly indicated that contact with carbon followed by oxidation leads to an agglomeration of barium particles (Fig. 7a and b). These barium agglomerates grow from 20 nm to 300 nm. Microscopy of $Pt–Ba/Al_2O_3$ (Fig. 7c) reveals that barium completely covered the support. The mean diameter of these agglomerates is close to 60 nm. Platinum particles are clearly identified with a diameter between 3 and 9 nm. In accordance to the results obtained for Pt/Al_2O_3 samples, aging of $Pt–Ba/Al_2O_3$ led to a large sintering of platinum and an increase in mean diameter to 25 nm. On the other hand, the alumina structure is clear while the barium particles are difficult to observe except on the edge of the catalyst particle.

Characterization of materials using TEM technology leads us to conclude that the oxidation of carbon in contact with the catalyst promotes Pt sintering and Ba agglomeration. These structural modifications reduce the proximity between Pt sites and adsorption sites (Ba and/or Al). This increased distance lowers NO_x storage by the 'nitrite route'.

4. Conclusion

The interaction between carbon and the model NSR catalysts was studied. The catalysts used were composed of Pt and/or Ba on Al_2O_3 (2%Pt/γ-Al_2O_3, 20%BaO/γ-Al_2O_3 and 2%Pt–20%BaO/γ-Al_2O_3). A comparison of NO_x storage capacity of the catalysts during NO_x adsorption/TPD cycles performed on catalysts alone or in the presence of a carbon–catalyst mixture (in a ratio equal to 6) was conducted. Adsorption phases were performed at 300 °C under a reactive gas composed of 300 ppm NO or NO_2 + 10% O_2. A carbon–catalyst contact was subsequently shown to decrease

the NSC regardless of the composition of the catalyst. However, this effect is more pronounced on Pt-free catalysts. Thus, contact between carbon and NO_x storage catalysts was suggested to primarily affect the nitrate species formed far from Pt (i.e., those formed by the "nitrate route"). A destabilization of these nitrate species then occurred via a direct surface reaction with carbon particles to form carbonate species. TPD profiles revealed that both Al and Ba sites were affected by this reaction. In addition, the carbon oxidation process led to premature aging of the catalysts and induced structure modifications (Pt sintering and Ba agglomeration). These structural modifications reduced the proximity between Pt and adsorption sites (Ba and/or Al), which resulted in decreased NO_x storage through the 'nitrite route'.

Acknowledgments

The authors thank the network REALISE (REseau Alsace de Laboratoire en Ingénierie et Sciences pour l'Environnement) for its financial support for equipment facilities. Financial support by the CNRS France is gratefully acknowledged by Ioana Fechete.

References

[1] J. Cooper, H.J. Jyung, J.E. Thoss, Treatment of diesel exhaust gases, US Patent 4,902,487, 1990.
[2] B. Stanmore, J.F. Brilhac, P. Gilot, Carbon 39 (2001) 2247–2268.
[3] B. Stanmore, V. Tschamber, J.F. Brilhac, Fuel 87 (2008) 131–146.
[4] F. Jacquot, V. Logie, J.F. Brilhac, P. Gilot, Carbon 40 (2003) 335–343.
[5] A. Setiabudi, M. Makkee, J.A. Moulijn, Applied Catalysis B 50 (2004) 185–194.
[6] M. Jeguirim, V. Tschamber, J.F. Brilhac, P. Ehrburger, Fuel 84 (14–15) (2005) 1949–1956.
[7] S.J. Jelles, M. Makkee, J.A. Moulijn, Topics in Catalysis 16 (2001) 269–273.
[8] M. Jeguirim, V. Tschamber, J.F. Brilhac, P. Ehrburger, Journal of Analytical and Applied Pyrolysis 72 (2004) 171–181.
[9] M. Jeguirim, V. Tschamber, P. Ehrburger, Applied Catalysis B 76 (2007) 235–240.
[10] M. Jeguirim, V. Tschamber, J.F. Brhillac, Journal of Chemical Technology & Biotechnology 84 (5) (2009) 770–776.
[11] L. Olsson, H. Persson, E. Fridell, M. Skoglundh, B. Andersson, Journal of Physical Chemistry B 105 (2001) 6895–6905.
[12] I. Nova, L. Castoldi, L. Lietti, E. Tronconi, P. Forzatti, F. Prinetto, G. Ghiotti, Journal of Catalysis 222 (2004) 377–388.
[13] H. Mazhoul, J.-F. Brilhac, P. Gilot, Applied Catalysis B 20 (1999) 47–55.
[14] P. Broqvist, H. Grönbeck, E. Fridell, I. Panas, Catalysis Today 96 (2004) 71–78.
[15] K. Nakatani, S., Hirota, S., Takeshima, K., Itoh, T. Tanaka, SAE paper SP-16742002-01-0957, 2002.
[16] C.N. Millet, R. Chedotal, P. Da Costa, Applied Catalysis B 90 (2009) 339–346.
[17] I. Pieta, M. Garcia-dieguez, C. Herrera, M. Larrubia, L.J. Alemany, Journal of Catalysis 270 (2010) 256–267.
[18] J. Klein, I. Fechete, V. Bresset, F. Garin, V. Tschamber, Catalysis Today 189 (2012) 60–64.
[19] R. Matarrese, N. Artioli, L. Castoldi, L. Lietti, P. Forzatti, Catalysis Today 184 (2012) 271–278.
[20] J. Sullivan, O. Keane, A. Cassidy, Applied Catalysis B 75 (2007) 102–106.
[21] K. Krishna, M. Makkee, Catalysis Today 114 (2006) 48–56.
[22] L. Castoldi, N. Artioli, R. Matarrese, L. Lietti, P. Forzatti, Catalysis Today 157 (2010) 384–389.
[23] N. Artioli, R. Matarrese, L. Castoldi, L. Lietti, P. Forzatti, Catalysis Today 169 (2011) 36–44.
[24] R.D. Clayton, M.P. Harold, V. Balakotaiah, C.Z. Wan, Applied Catalysis B 90 (2009) 662.
[25] D. Bhatia, M.P. Harold, V. Balakotaiah, Catalysis Today 151 (2010) 314.
[26] B.S. Sanchez, C.A. Querini, E.E. Miro, Applied Catalysis A 366 (2009) 166–175.